PIBB 生物化学与生物物理进展
Progress in Biochemistry and Biophysics
2020,47(11):1199~1206
www.pibb.ac.cn

Purification and Characterization of the Protein Complex Formed by Microcephaly Protein ASPM and Calmodulin*

CHANG Meng-Yuan[1,2], WEI Xiao-Xi[1,2], LU Qing[1,2]**

([1])*Bio-X-Renji Hospital Research Center, Renji Hospital, School of Medicine, Shanghai Jiao Tong University, Shanghai* 200127, China;
[2])*Key Laboratory for the Genetics of Developmental and Neuropsychiatric Disorders, Bio-X Institutes, Ministry of Education, Shanghai Jiao Tong University, Shanghai* 200230, China)

Abstract Autosomal recessive primary microcephaly is a neurodevelopmental disorder associated with reduced brain size and intellectual disability. *ASPM* (abnormal spindle-like microcephaly-associated) is the most common recessive microcephaly gene, but the underlying mechanism is poorly understood. Here, we show that calmodulin function as a vital regulator of ASPM by interacting with its IQ-region. The complex of ASPM IQ-region and apo_calmodulin was purified and biochemically characterized with a 1:8 stoichiometry by size exclusion chromatography coupled with multi-angle static light scattering (SEC-MALS) and circular dichroism spectroscopy (CD). Interestingly, the binding ratio of ASPM IQ-region with Ca^{2+}_calmodulin changed to 1:7 in the presence of Ca^{2+}. In addition, by comparing the CD spectra with and without Ca^{2+}, the ASPM-Calmodulin complex showed Ca^{2+}-dependent thermal stability change. Taken together, these results suggested a Ca^{2+}-induced regulation mechanism of ASPM-calmodulin interaction.

Key words microcephaly, ASPM, CaM, Ca^{2+}, interaction
DOI: 10.16476/j.pibb.2020.0138

1 Introduction

Microcephaly is a neurodevelopmental disorder characterized by small brain and intellectual disability[1-2]. Autosomal recessive primary microcephaly (MCPH) is associated with mutations of at least 18 genes[2-4]. Among them, *ASPM* gene is most frequently mutated in microcephaly[1-2]. More than half of the MCPH mutations occurred on ASPM, while the mutations occurred on the other 17 genes were less than 40% as reported[1]. Zika virus (ZIKV) raised global concern to microcephaly[5]. Research data showed that several microcephaly genes were down-regulated (*ASPM, CASC5, CENPF, MCPH1, RBBP8, STIL, TBR2*) after ZIKV infection, among which *ASPM* was down-regulated to the greatest extent[6-7]. ASPM and many other microcephaly proteins were reported to be involved in spindle assembly during mitosis for neuronal development[8-11], but the detailed molecular mechanism is largely unknown.

From its N to C terminus, ASPM contains two calponin homology (CH) domains for cytoskeleton association[12], a large region made up of ~ 50 isoleucine-glutamine (IQ) motifs and a conserved C-terminal tail (Figure 1a). IQ motifs usually locate in the neck region of members from the myosin superfamily and function as the lever arm for myosin motor[13]. Myosin member normally contains about 3-6 IQ motifs[14-15] while mammalian ASPM has such a huge number of IQ motifs with unidentified function. Calmodulin (CaM) can interact with myosin IQ motifs in a Ca^{2+}-regulated manner. Apo_CaM (Ca^{2+}-free state) specifically binds to and maintains the conformational rigidity of the IQ motifs[16-18]. An

* This work was supported by grants from The National Natural Science Foundation of China (31900858) and Shanghai Sailing Program (18YF1410600).
** Corresponding author.
Tel:86-13023155837, E-mail: luqing67@sjtu.edu.cn
Received: May 12, 2020 Accepted: June 18, 2020

increase of cellular Ca^{2+} concentration will weaken the interaction between CaM and IQ motifs and thereby cause CaM to dissociate from myosins[18-19]. While it should be pointed out that several IQ motifs in myosins can bind with both apo_CaM and Ca^{2+}_CaM[15,17]. However, studies on the interaction between IQ motifs and CaM have been limited to IQ motifs from myosin proteins and the binding mode between IQ-rich region of ASPM and CaM is lack of detailed investigation.

ASPM plays a vital role in the mitotic process of neural progenitor cells (NPCs) [20-22]. In *Drosophila*, Asp (ortholog of ASPM in *Drosophila*) accumulates at spindle pole during the prometaphase to middle stages of cell mitosis and is essential for spindle assembly[23]. CaM also participates in this process by working along with Asp[24]. They co-localize at spindle pore and form the protein complex to cross-link the spindle microtubules. Disrupting the interaction of Asp-CaM will cause the spindle pole un-focusing and the detachment from the centrosome[24]. Previous research has found that, for Asp from Drosophila, IQ-rich region can interact with CaM[23-24]. However, whether Ca^{2+} signal can regulate Asp-CaM complex formation is still unknown and studies from different species will provide insight into the function of ASPM for brain evolution.

In this study, we purified and biochemically characterized the protein complex formed by the conserved IQ-region of mouse ASPM with calmodulin. With the help from the co-expression system in *Escherichia coli*. (*E. coli*.), we could obtain soluble IQ fragments (F1: amino acid 2 589 to 2 870 & F2: 2 673 to 2 870) of ASPM in complex with apo-calmodulin. Size exclusion chromatography coupled with multi-angle static light scattering (SEC-MALS) results showed that the binding ratios are 1∶8 for ASPM_F1/apo_CaM and 1∶6 for ASPM_F2/apo_CaM. More interesting, an increase of Ca^{2+} caused the dissociation of one copy CaM and change of the binding ratio to 1∶7 for ASPM_F1/Ca^{2+}_CaM and 1∶5 for ASPM_F2/Ca^{2+}_CaM. Furthermore, the circular dichroism studies demonstrated that all of the protein complexes exhibited typical α-helical folding features. Finally, ASPM/CaM complexes showed Ca^{2+}-dependent thermal stability change.

2 Materials and methods

2.1 Constructs, protein expression and purification

Two constructs for ASPM IQ region were PCR amplified from the mouse full length ASPM (NP_033921.3) and cloned into a pET-32m3C-CoEx vector respectively. The pET-32m3C-CoEx vector contains two ribosome binding sites for protein co-expression, engineered from pET-32a vector. Human CaM (NP_008819.1) were cloned to the same pET-32m3C-CoEx vector for co-expression with ASPM fragments respectively. These two ASPM/CaM complexes were co-expressed in BL21 *Escherichia coli* cells. Protein expression was induced by addition of IPTG at 16℃ for 24 h. The His-tagged proteins were purified by Ni^{2+}-NTA agarose affinity chromatography followed by size-exclusion chromatography using the column buffer of 50 mmol/L Tris-HCl, pH 7.8, containing 100 mmol/L NaCl, 1 mmol/L DTT, and 10 mmol/L EDTA (EDTA buffer) or 50 mmol/L Tris-HCl, pH 7.8, containing 100 mmol/L NaCl, 1 mmol/L DTT, and 10 mmol/L $CaCl_2$ ($CaCl_2$ buffer).

2.2 Static light scattering analysis

Protein samples (160 μl at a concentration of 20 μmol/L) was injected into a Superose 12 (10/300 GL) column (GE Healthcare) equilibrated with EDTA buffer or $CaCl_2$ buffer. The AKTA FPLC system was coupled to a three-angle light-scattering detector (miniDAWN TREOS, Wyatt technology) and a refractive index detector (Optilab T-rEX, Wyatt technology). The data were recorded and processed by the ASTRA 6.1.2 software (Wyatt Technology).

2.3 Circular dichroism (CD) spectra measurements

Circular dichroism spectra were obtained by using a Chirascan instrument with a cell holder. Spectra were recorded from 200 to 240 nm with two repeats using a quartz cell of 0.5 mm light path. The final concentration of protein samples was 0.03 mmol/L in buffers containing 5 mmol/L Tris-HCl (pH 7.8), 10 mmol/L NaCl, 0.1 mmol/L DTT, with 1 mmol/L EDTA or 1 mmol/L $CaCl_2$. Each CD spectrum was subtracted by the buffer blank first. The temperature ranges from 20 degrees Celsius to 80 degrees Celsius, and a curve was made every ten degrees Celsius.

2.4 Microplate reader for the measurement of the complex concentration

Trx-tagged protein was used as a standard, and the light absorption at 595 nm of the four concentration gradient complexes was determined by Bradford method using a microplate reader to calculate the precise mass concentration of the complexes. Nanodrop was used to measure the light absorption of the complex at UV280. There is a formula that can calculate the molar extinction coefficient(ε) based on absorbance(A) and concentration(C). The formula is $A = \varepsilon CL$ (L stands for liquid layer thickness, here is 1 cm). Finally, we used these two values to calculate the molar extinction coefficient of the complexes.

2.5 The calculation of the binding stoichiometry of ASPM and CaM

To determine the binding ratio of ASPM and CaM, we obtained the molar extinction coefficient and the molecular mass of ASPM-CaM complex and then listed a system of linear equations: $m\varepsilon_A + n\varepsilon_B = \varepsilon_{A+B}$, $mM_A + nM_B = M_{A+B}$. (M stands for molecular mass, A&B stands for protein ASPM&CaM, A+B stands for the complex of ASPM and CaM). After that, the two coefficients m and n which represent the binding stoichiometry of ASPM and CaM can be calculated according to the two equations.

2.6 Homology modeling

Modeling templates were identified in the Protein Data Bank (PDB). The initial homology model was built based on Myo7a/apo_CaM (PDB 5WSU) and Myo7a/Ca^{2+}_CaM (PDB 5WSV) using SWISS-MODEL server. The quality of the final structure model was validated using VERIFY3D. For the model of ASPM_IQ1/apo_CaM, 93.02% of the residues had an averaged 3D-1D score >0.2. For the model of ASPM_IQ1/Ca^{2+}_CaM, 80.45% of the residues had an averaged 3D-1D score >0.2.

3 Results

3.1 The IQ−region of ASPM can form a stable complex with apo−calmodulin

The number of IQ motifs in ASPM varies markedly between species, but the C-terminal IQ-region is evolutionarily conserved among the vertebrates (Figure 1a). The C-terminal conserved IQ-rich fragment of mouse ASPM starts from amino acid 2 589 to 2 870, named as ASPM_F1. The second fragment from amino acid 2 673 to 2 870 was also tested in this study and named as ASPM_F2. Previous study assumed that there were only 5 IQ motifs in the region of ASPM_F1. Based on structure/sequence alignment, we predicted that there are 8 IQ motifs in ASPM_F1 (IQ1-IQ8 in Figure 1b) and 6 IQ motifs in ASPM_F2 (IQ3-IQ8 in Figure 1b). Sequence alignments and secondary structure predictions suggest that each IQ-motif has the characteristic sequence as "IQXXXR" for apo_CaM binding. The positions of the residues of IQ-region which may be involved in anchoring Ca^{2+}_CaM were also highlighted in red box, including two hydrophobic residues at positions "+3", "+7" and positive-charged residue at position "+11" (the Ile in the signature "IQ" sequence in each IQ motif is defined as the position "0"). However, due to the remarkable capacity of Ca^{2+}_CaM binding, it is highly possible for Ca^{2+}_CaM to

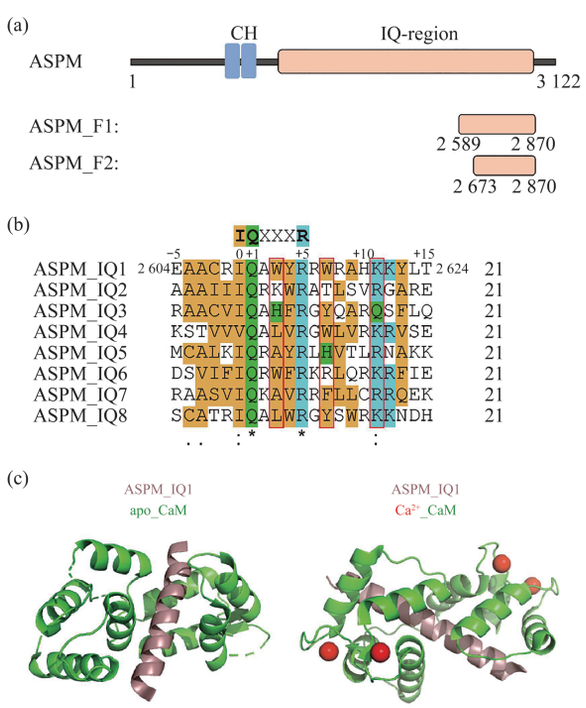

Fig. 1 Sequence and structure analysis on IQ−region of ASPM

(a) Domain organizations of full-length ASPM. CH: calponin homology domain; IQ: isoleucine-glutamine motif. ASPM_F1: Fragment 1 of ASPM starting from amino acid 2 589 to 2 870; ASPM_F2: Fragment 2 of ASPM starting from amino acid 2 673 to 2 870. (b) Sequence alignment of IQ motifs that can interact with CaM tested in this study. The red box highlights the positions of the residues critical for anchoring Ca^{2+}_CaM. (c) Predicted structure models of ASPM_IQ1/apo_CaM (left) and ASPM_IQ1/Ca^{2+}_CaM (right) (based on Myo7a/apo_CaM PDB 5WSU and Myo7a/Ca^{2+}_CaM PDB 5WSV).

use other positions (eg. position "0" and "9") as anchoring points. In order to gain more information on the structural features, we built the structure models of ASPM_IQ1 in complex with apo_CaM and Ca^{2+}_CaM (Figure 1c), using homology modeling. The initial homology model was built based on Myo7a/apo_CaM (PDB: 5WSU) and Myo7a/Ca^{2+}_CaM (PDB: 5WSV) using SWISS-MODEL server. Our model of ASPM_IQ1/apo_CaM (Figure 1c left) showed that IQ1 can bind to apo-CaM in a canonical fashion, with the C-terminal lobe of CaM adopting a semi-open conformation (anchored by the signature Ile residue of the "IQ" motif) and the N lobe adopting a closed conformation. In Figure 1c right, Ca^{2+}_CaM binds to IQ1 with the N lobe of CaM interacting with the N-terminal half of IQ1 and the C lobe interacting with the C-terminal half of IQ1. In the presence of Ca^{2+}, the EF hands in both lobes of CaM adopt a typical open conformation, resulting in a highly compact complex structure similar to many other well-studied Ca^{2+}_CaM/target complexes.

To test whether the ASPM can form a stable complex with CaM, we got ASPM_F1 and ASPM_F2 protein co-expressed with apo_CaM in the absence of Ca^{2+}. Isolated ASPM fragments were insoluble in tested conditions, so we used the *E. coli* co-expression system to purify ASPM/CaM complexes. In Figure 2a and b, co-migration of ASPM with CaM on SDS-PAGE indicated the complex formation between these two proteins. And the symmetric peak of UV spectrum suggested the proteins complexes are both highly homogeneous. Taken together, IQ-fragments ASPM_F1 and ASPM_F2 with apo_CaM can both form stable and homogeneous complexes in solution.

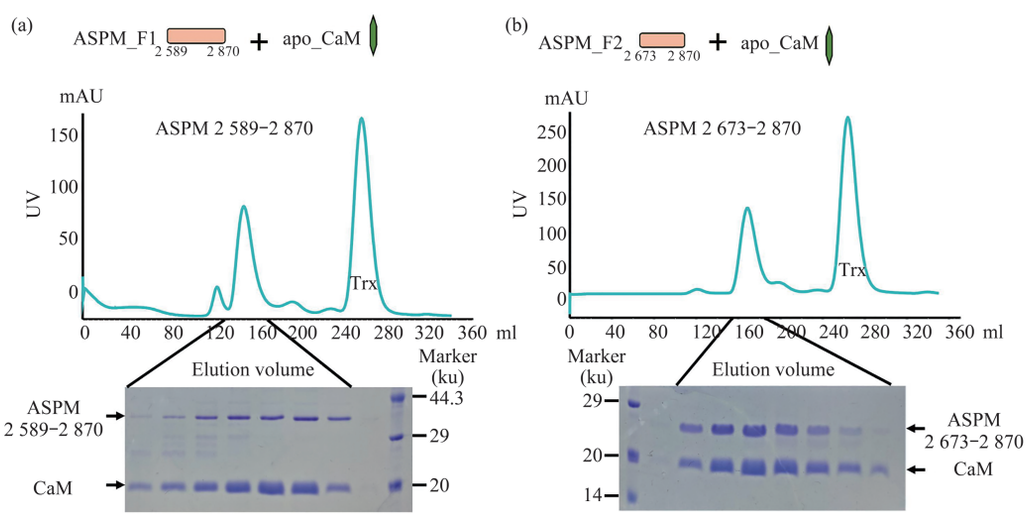

Fig. 2 The IQ−region of ASPM can form a stable complex with CaM

The purification profiles of ASPM/CaM complex by gel-filtration chromatography in 10 mmol/L EDTA buffer. UV 280 nm peak and SDS-PAGE showing the co-migration of ASPM_F1/apo_CaM in (a) and ASPM_F2/apo_CaM in (b). The latter peak of A&B is Trx protein.

3.2 The binding ratio of IQ_ASPM/Calmodulin complex

To determine the binding stoichiometry, size exclusion chromatography coupled with multi-angle static light scattering (SEC-MALS) was used to analyze IQ_ASPM/CaM complexes in EDTA buffer and $CaCl_2$ buffer. Measured molecular weight of ASPM_F1/CaM complex was fitted to about 179 ku, suggesting ASPM_F1/CaM in 1∶*n* binding stoichiometry (Figure 3a). The molecular weight of the shorter fragment ASPM_F2 in complex with CaM is 121 ku (Figure 3b), ~ 50 ku less than ASPM_F1, which match the theoretical mass of 2 CaMs plus a 2 589−2 673 of ASPM (Supplementary Table S1). The results indicated that the binding ratios may be 1∶*n* for ASPM_F1/CaM and 1∶(*n*-2) for ASPM_F2/CaM. To further substantiate this conclusion, extinction coefficient of protein complex was measured to

determine the binding stoichiometry, by performing Bradford assay coupled with UV-280nm absorbance measurement (Supplementary Table S2). The results showed that the binding ratios are 1∶8 for ASPM_F1/apo_CaM and 1∶6 for ASPM_F2/apo_CaM (Figure 3c), consistent with our prediction (Figure 1b).

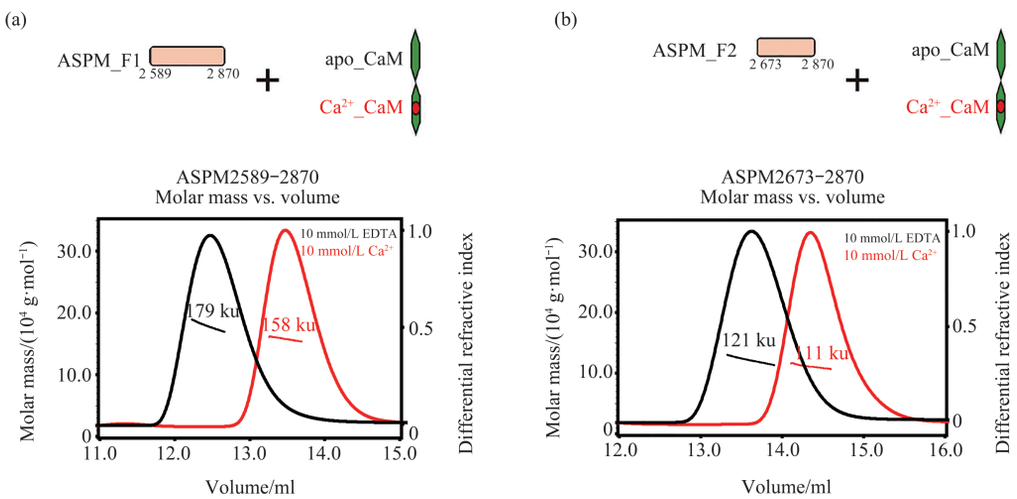

(c)

Protein	Molar mass ($CaCl_2$)	ASPM：CaM	Molar mass (EDTA)	ASPM：CaM
ASPM (2589−2870)	158 ku	1 ：7	179 ku	1 ：8
ASPM (2673−2870)	111 ku	1 ：5	121 ku	1 ：6

Fig. 3 The binding stoichiometry between ASPM and CaM

(a, b) Size exclusion chromatography coupled with multi-angle static light scattering (SEC-MALS), showing the molecular mass of ASPM/apo_CaM (black) complex and ASPM/Ca^{2+}_CaM (red) complex. ASPM_F1 in (a); ASPM_F2 in (b). (c) The molecular mass of ASPM/CaM complexes and the binding stoichiometry calculated. The binding stoichiometry changed in the presence of Ca^{2+}.

3.3 Ca^{2+}−induced binding change of ASPM/Calmodulin complexes

To test whether Ca^{2+} would affect the binding between ASPM IQ-region with CaM, ASPM_F1/CaM and ASPM_F2/CaM protein complexes were characterized by SEC-MALS in the presence of Ca^{2+}. Measured molecular weights of ASPM_F1/Ca^{2+}_CaM ASPM_F2/Ca^{2+} _CaM are 158 ku and 111 ku in 10 mmol/L $CaCl_2$, indicating a ~17 ku decrease of molar mass caused by Ca^{2+} (Figure 3a,b). The binding ratios are 1∶7 for ASPM_F1/ Ca^{2+}_CaM and 1∶5 for ASPM_F2/ Ca^{2+} _CaM (Figure 3c). Taken together, the increase of Ca^{2+} concentration caused the dissociation of one copy CaM from C-terminal IQ-region of ASPM, which suggested that Ca^{2+} signaling may be involved in regulating ASPM/CaM function in brain development.

As showed by the biochemical results, both ASPM_F1(covering IQ1-IQ8) and ASPM_F2 (covering IQ3-IQ8) lost one calmodulin in the presence of Ca^{2+}, so one of the IQs in IQ3-IQ8 would be responsible for Ca^{2+}_CaM dissociation. Based on sequence analysis (Figure 1b), two hydrophobic residues at positions "+3", "+7" and positive-charged residue at position " +11" may be involved in Ca^{2+}_CaM binding. IQ3 with His at position "+3" and Gln at position "+11" may not be able to maintain Ca^{2+} _CaM with high affinity. Another candidate would be IQ6 with Arg at position " +7". The exact binding modes of these IQ motifs will need further biochemical and structural characterization.

3.4 ASPM/ Calmodulin complexes showed Ca^{2+}−dependent thermal stability change

To further test whether Ca^{2+} will induce other structural change of ASPM/CaM complex, circular dichroism (CD) spectra of ASPM_F1/CaM and

ASPM_F2/CaM were recorded with or without Ca^{2+} (Figure 4a2, a3, b2, b3) under various temperature. At room temperature, consistent with structure prediction (Figure 1c), CD spectra showed that the protein complexes are all largely α-helical with or without Ca^{2+}. But increase of Ca^{2+} caused a dramatic change of thermal stability of the ASPM/CaM complex, when thermal denaturation were performed under the temperature from 20℃−80℃. The ellipticity value of the characteristic peak for α-helix at 222 nm was selected as a representative to generate denaturation curve. As shown in Figure 4a1, b1, the denaturation curves showed that ASPM/CaM complexes have greater stability in the presence of Ca^{2+}, compared with Ca^{2+}-free condition. Our results indicated that Ca^{2+} may regulate ASPM/CaM function by inducing conformational change of complex structure.

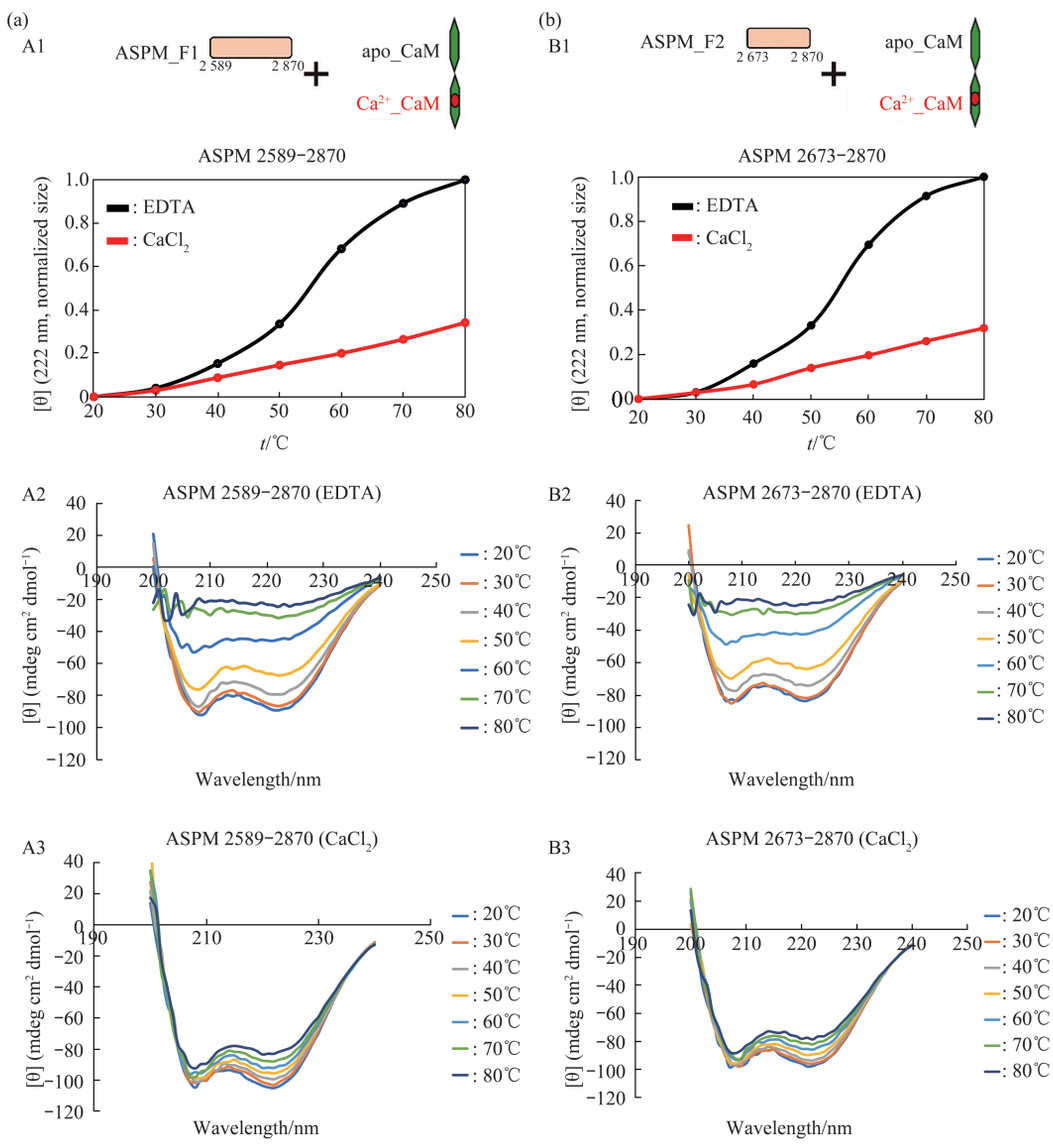

Fig. 4　ASPM/CaM complexes showed greater stability in the presence of Ca^{2+}

(A1, B1) Thermal denaturation profiles of ASPM/CaM complex in the absence of Ca^{2+}(black) and the presence of Ca^{2+}(red) by plotting the ellipticity values of the protein at 222 nm as a function of temperature. (A2, A3, B2, B3) Circular dichroism spectra of ASPM/CaM complexes with and without Ca^{2+} at different temperatures (from 20℃ to 80℃). ASPM_F1 in (a); ASPM_F2 in (b).

4 Discussion

ASPM is an important microcephaly gene, which plays a vital role whether for hereditary microcephaly or microcephaly caused by Zika virus[1,6,8]. ASPM participates in brain development by affecting the cell division of neural progenitor cells. CaM is also indispensable in this process[23-24]. Previous research found that the IQ-rich domain of ASPM interacts with CaM[23-24], while the specific mechanism of interaction is unknown. In this study, our data showed that the conserved IQ-fragment of ASPM can interact with calmodulin with a binding ratio of 1∶8 and furthermore the complex formation can be regulated by Ca^{2+} signal. First, the protein complex of ASPM_F1/apo_CaM contains up to eight copies of calmodulin (Figure 3a, c), which is much more than myosin/calmodulin complex reported before (only 3–6 copies of calmodulin[14]). Given that calmodulin is the most versatile and universal Ca^{2+} signal modulator, this newly discovered calmodulin/target binding mode may be applied to other calmodulin association proteins. Second, purification and biochemical characterization of ASPM/calmodulin protein complex offers the first mechanistic insights into how calmodulin can interact with IQ-region of ASPM in a Ca^{2+}-regulated manner. Thus, the complex formation of ASPM and calmodulin under Ca^{2+} regulation can serve as a blueprint for understanding how ASPM and calmodulin involved in brain development.

Supplementary material 20200138_Supple Table S1 and S2. pdf are available at paper online (http://www.pibb.ac.cn or http://www.cnki.net)

References

[1] Kaindl A M, Passemard S, Kumar P, *et al*. Many roads lead to primary autosomal recessive microcephaly. Progress in Neurobiology, 2010, **90**(3): 363-383

[2] Verloes A, Drunat S, Passemard S. ASPM Primary Microcephaly. 2020 Apr 2. In: Adam MP, Ardinger HH, Pagon RA, *et al*., editors. GeneReviews® [Internet]. Seattle (WA): University of Washington, Seattle; 1993-2020

[3] Naveed M, Kazmi S K, Amin M, *et al*. Comprehensive review on the molecular genetics of autosomal recessive primary microcephaly (MCPH). Genetics Research, 2018, **100**: e7

[4] Létard P, Drunat S, Vial Y, *et al*. Autosomal recessive primary microcephaly due to ASPM mutations: an update. Human Mutation, 2018, **39**(3): 319-332

[5] Barreto M L, Barral-Netto M, Stabeli R, *et al*. Zika virus and microcephaly in Brazil: a scientific agenda. Lancet, 2016, **387**(10022): 919-921

[6] Li C, Xu D, Ye Q, *et al*. Zika virus disrupts neural progenitor development and leads to microcephaly in mice. Cell Stem Cell, 2016, **19**(1): 120-126

[7] Tang H, Hammack C, Ogden S C, *et al*. Zika virus infects human cortical neural progenitors and attenuates their growth. Cell Stem Cell, 2016, **18**(5): 587-590

[8] Johnson M B, Sun X, Kodani A, *et al*. Aspm knockout ferret reveals an evolutionary mechanism governing cerebral cortical size. Nature, 2018, **556**(7701): 370-375

[9] Jayaraman D, Kodani A, Gonzalez D M, *et al*. Microcephaly proteins Wdr62 and Aspm define a mother centriole complex regulating centriole biogenesis, apical complex, and cell fate. Neuron, 2016, **92**(4): 813-828

[10] Jiang K, Rezabkova L, Hua S, *et al*. Microtubule minus-end regulation at spindle poles by an ASPM – katanin complex. Nature Cell Biology, 2017, **19**(5): 480-492

[11] Akhmanova A, Steinmetz M O. Microtubule minus-end regulation at a glance. J Cell Sci, 2019, **132**(11): jcs227850

[12] Gimona M, Djinovic-Carugo K, Kranewitter W J, *et al*. Functional plasticity of CH domains. FEBS Letters, 2002, **513**(1): 98-106

[13] Vale R D. The molecular motor toolbox for intracellular transport. Cell, 2003, **112**(4): 467-480

[14] Liu J, Taylor D W, Krementsova E B, *et al*. Three-dimensional structure of the myosin V inhibited state by cryoelectron tomography. Nature, 2006, **442**(7099): 208-211

[15] Sakai T, Jung H S, Sato O, *et al*. Structure and regulation of the movement of human myosin VIIA. Journal of Biological Chemistry, 2015, **290**(28): 17587-17598

[16] Houdusse A, Gaucher J F, Krementsova E, *et al*. Crystal structure of apo-calmodulin bound to the first two IQ motifs of myosin V reveals essential recognition features. Proc Natl Acad Sci USA, 2006, **103**(51): 19326-19331

[17] Li J, Chen Y, Deng Y, *et al*. Ca^{2+}- induced rigidity change of the myosin VIIa IQ motif-single α helix lever arm extension. Structure, 2017, **25**(4): 579-591.e574

[18] Lu Q, Li J, Ye F, *et al*. Structure of myosin-1c tail bound to calmodulin provides insights into calcium-mediated conformational coupling. Nature Structural & Molecular Biology, 2015, **22**(1): 81-88

[19] Heissler S M, Sellers J R. Myosin light chains: teaching old dogs new tricks. Bioarchitecture, 2014, **4**(6): 169-188

[20] Fujimori A, Itoh K, Goto S, *et al*. Disruption of Aspm causes microcephaly with abnormal neuronal differentiation. Brain and Development, 2014, **36**(8): 661-669

[21] Fish J L, Dehay C, Kennedy H, *et al*. Making bigger brains-the evolution of neural-progenitor-cell division. J Cell Sci, 2008, **121**(Pt17): 2783-2793

[22] Higgins J, Midgley C, Bergh A M, *et al*. Human ASPM participates in spindle organisation, spindle orientation and cytokinesis. BMC Cell Biology, 2010, **11**: 85

[23] Ito A, Goshima G. Microcephaly protein Asp focuses the minus ends of spindle microtubules at the pole and within the spindle. The Journal of Cell Biology, 2015, **211**(5): 999-1009

[24] Schoborg T, Zajac A L, Fagerstrom C J, *et al*. An Asp-CaM complex is required for centrosome-pole cohesion and centrosome inheritance in neural stem cells. The Journal of Cell Biology, 2015, **211**(5): 987-998

小脑症蛋白ASPM和钙调蛋白复合物的纯化和表征*

常梦园[1,2] 魏晓西[1,2] 陆 青[1,2)**

([1]) 上海交通大学医学院附属仁济医院Bio-X仁济医院研究中心，上海 200127；

[2)] 上海交通大学，Bio-X研究院，遗传发育与精神神经疾病重点实验室，上海 200230）

摘要 常染色体隐性小脑症（autosomal recessive primary microcephaly，MCPH）是一种与大脑缩小和智力缺陷有关的神经发育障碍. ASPM（abnormal spindle-like microcephaly-associated）是最常见的MCPH致病基因，但其潜在机制尚不清楚. 研究发现，钙调蛋白（calmodulin，CaM）通过与ASPM的IQ区域相互作用而对ASPM的功能有重要调控作用. 我们纯化了ASPM IQ区域和CaM的复合物，并通过分子排阻色谱结合多角度静态光散射（SEC-MALS）和圆二光谱（CD）实验发现，ASPM和apo_CaM的结合比例为1∶8. 有趣的是，在Ca^{2+}存在时，ASPM的IQ区域与Ca^{2+}_CaM的结合比例变为了1∶7. 此外，通过比较不同条件下（Ca^{2+}存在与否）的CD光谱，ASPM-CaM复合物显示出Ca^{2+}依赖性的热稳定性变化. 综上所述，该研究揭示了Ca^{2+}诱导的ASPM-CaM相互作用的调节机制.

关键词 小脑症，ASPM，CaM，Ca^{2+}，相互作用

中图分类号 Q51 **DOI**：10.16476/j.pibb.2020.0138

* 国家自然科学基金（31900858）和上海市扬帆计划（18YF1410600）资助项目.

** 通讯联系人.

Tel：13023155837，E-mail：luqing67@sjtu.edu.cn

收稿日期：2020-05-12，接受日期：2020-06-18